Pergamon

SCIENCE DIRECT®

Tetrahedron 59 (2003) 5495–5506

TETRAHEDRON

# Synthesis and optical properties of conjugated dendrimers with unsymmetrical branching

Yongchun Pan,[a] Zhonghua Peng[a,*] and Joseph S. Melinger[b]

[a]*Department of Chemistry, University of Missouri—Kansas City, 5100 Rockhill Road, Kansas City, MO 64110, USA*
[b]*Naval Research Laboratory, Electronics Science and Technology Division, Code 6812, Washington, DC 20375, USA*

Received 9 April 2003; revised 27 May 2003; accepted 27 May 2003

**Abstract**—An improved synthetic approach to conjugated monodendrons with unsymmetrical branching structures is reported. Dendrimers containing two or three such conjugated monodendrons are synthesized and their optical properties are studied. Such dendrimers exhibit broad absorptions and very high fluorescence quantum yields, making them promising candidates for applications in molecular-based photonics. 

## 1. Introduction

Dendrimers are hyperbranched macromolecules with a branching structure that may be described as tree-like.[1] Dendrimers are characterized by unique structural features such as a high density of peripheral sites, a convergent periphery-to-core branching structure, and, for sufficiently large generations, a globular-like three-dimensional shape. These features suggest that dendrimers are good candidates for light-harvesting applications.[2–4] Indeed, numerous light-harvesting dendrimers have been reported. One class of light harvesting dendrimers utilize dendritic branches as scaffolds on which to anchor light-absorbing chromophores.[2–3] Another class uses π-conjugated branches as both the light-absorbing units and energy transport medium.[4,5] The π-conjugated branches are usually linked through the *meta* positions of phenyl rings, which interrupts inter-branch π-conjugations. As a result, the electronic excitations are localized on individual branches.[4–6] One example is the compact phenylacetylene (PA) monodendron synthesized and studied by Moore, Kopelman, and co-workers.[4,6] The PA monodendron is structurally symmetric, resulting from substitution entirely at the *meta*-positions of the benzene ring. Recently, we reported a light-harvesting monodendron based on an unsymmetrical branching frame where conjugated branches are linked through the *meta* and the *para* positions.[7] Such a dendron not only exhibits broad absorptions, but also possesses an intrinsic energy gradient from the surface branches to the core, resulting in efficient and ultrafast energy funneling properties.[8] In this paper, we report the detailed and improved synthesis of such unsymmetrical PA monodendrons. Further, by taking advantage of the phenol group at the dendron locus, larger dendrimers with two or three unsymmetrical PA monodendrons are prepared. The detailed synthesis, structural characterizations, and optical properties of such dendrimers are discussed.

## 2. Results and discussion

### 2.1. Synthesis of monodendrons

Our previous synthetic approach utilizes compound **I** as the building block molecule, and monodendrons up to the fourth generation have been synthesized according to Scheme 1.[7]

Since compound **I** is the building block molecule, its facile, efficient and large-scale synthesis is desirable. Scheme 2 shows such an efficient synthetic pathway to compound **I**. We have previously reported using $BBr_3$ as the monodemethylation agent to convert compound **3** to **4**,[7] which gave only about 40% yield. Although using *B*-bromo-9-BBN, selective demethylation of one of the methoxy groups could be achieved in 81% yield (Scheme 2),[9] the reaction is rather slow and the starting material never disappeared.[9–10] About 5% of starting material was recovered after the reaction mixture was refluxed for 3 days. It is advised not to increase the ratio of *B*-Br-9-BBN to the substrate. Additional *B*-Br-9-BBN gave noticeably more of the dihydroxy side product. It was thus desirable to introduce another protective group that is stable enough to withstand the vigorous iodination conditions and yet can be easily removed afterwards. We have chosen the isopropyl group since it has been shown that isopropyl aryl ethers can be

*Keywords*: dendrimers; fluorescence; light-harvesting.
* Corresponding author. Tel.: +1-816-235-2288; fax: +1-816-235-5502; e-mail: pengz@umkc.edu

0040–4020/03/$ - see front matter 
doi:10.1016/S0040-4020(03)00827-5

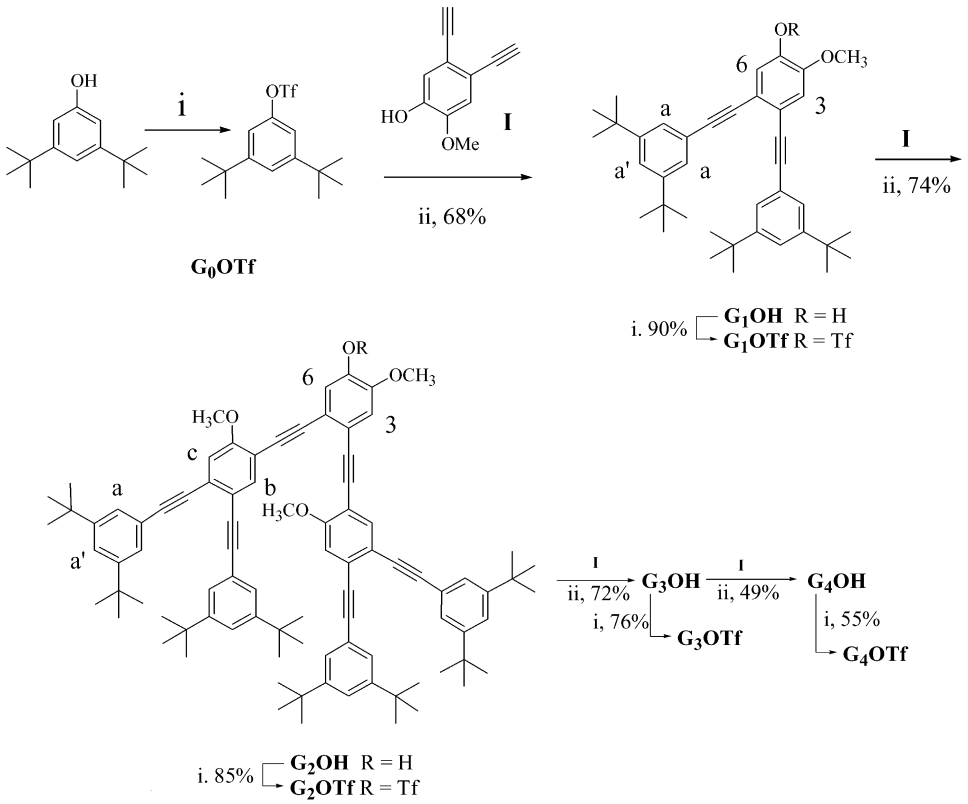


**Scheme 1.** Synthesis of monodendrons: (i) $(CF_3SO_2)_2O$, pyridine, 0°C; (ii) $PdCl_2(PPh_3)_2$, $NEt_3$, DMF, 65°C.

selectively cleaved by boron trichloride or aluminum trichloride under mild conditions while methyl aryl ethers were left intact.[11] Thus, compound **2** was synthesized in 2 steps from 2-methoxylphenol (Scheme 2) in excellent yields. Treatment of **2** with aluminum trichloride[11b] at room temperature resulted in an unidentified mixture including the unreacted starting material. However, the reaction of **2** with 1.05 equiv. of *B*-Br-9-BBN (1 M in methylene chloride) at reflux temperature went smoothly. Most of the starting material was consumed in only 1 h. After simple acid/base extraction, 4,5-diiodo-2-methoxyphenol was obtained in 92% yield. This procedure allows simple and efficient synthesis of 4,5-diiodo-2-methoxyphenol on large scale (~100 g).

**G1OH**, as illustrated in Scheme 1, was initially synthesized by a coupling reaction of compound **I** with 3,5-bis(*tert*-butyl)phenol triflate (**G0OTf**). The reaction proceeded without the protection of the hydroxy group, which greatly simplified the synthesis, and the product can be easily separated from the unreacted triflate **G0OTf** due to the presence of the polar hydroxy group in the product. This strategy using unprotected phenol as the monomer offers an additional advantage when compared to the coupling reaction using aryl halides. The diacetylene side product resulting from the homocoupling reaction of terminal alkynes, if ever formed, has significantly different polarity than the desired product and can thus be easily separated. Unfortunately, compound **I**, with an enediyne structure, is

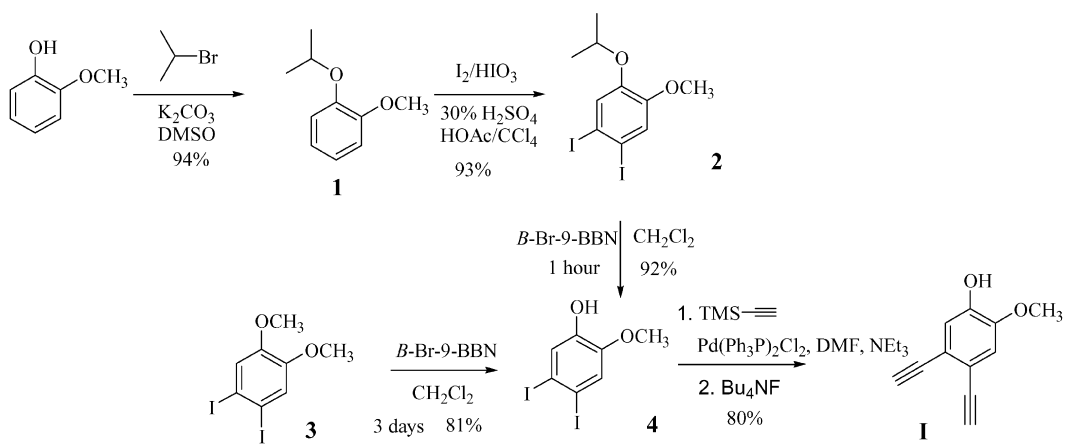


**Scheme 2.** Improved synthesis of 4,5-diiodo-2-methoxyphenol **4**.

temperature sensitive and appears not to be very stable under the reaction conditions. One possible side reaction is the Bergman cyclization reaction of enediyne.[12] It is also possible that compound **I** reacted with itself to form a polymeric material, as evidenced by our attempt to synthesize 4-ethynylphenol. Upon treatment of 4-trimethylsilylethynylphenol, a quite stable compound, with *tert*-butylammonium fluoride, the product, 4-ethynylphenol, decomposed quickly during chromatography and solvent evaporation to give a black tar-like material. Because of the side reactions, excess compound **I** has to be used in each coupling step. Even so, there is still a significant amount of triflate recovered (yields shown in Scheme 1 are calculated based on triflates reacted).

To circumvent using enediyne **I** directly, one strategy is to generate alkyne in situ.[13] Thus, 4,5-bis[(trimethylsilyl)-ethynyl]-2-methoxyphenol was heated with $K_2CO_3$, **G0OTf**, and dichlorobis(triphenyl)palladium(II) in methanol. However, the reaction was not complete and a complicated mixture including the desired product was obtained.

To avoid using enediyne **I**, we turned to an alternative route using 4,5-diiodo-2-methoxyphenol **4** as the building block molecule. As shown in Scheme 3, the Sonogashira Coupling of compound **4** with slightly over 2 equiv. of 3,5-di-*tert*-butylphenylacetylene gave **G1OH** in excellent yields.[14] The conversion of **G1OH** to **G1OTf** is efficient. Taking advantage of the relative reactivity of iodo versus triflate, **G1OTf** can be synthesized in a single step by the coupling reaction of **4** with 4,5-diiodo-2-methoxyphenol triflate (**II**).[15] The disadvantage of this procedure is that it is difficult to isolate the product **G1OTf** from the diacetylene byproduct and the unreacted compound **II**. The conversion of **G1OTf** to G1-acetylene compound **G1A** is very efficient. However, the coupling of **G1A** with either **4** or **II** gives very poor yields, presumably due to the severe steric hindrance at the two *ortho* reaction sites. By comparing the two possible routes, we conclude that the strategy using coupling reactions of compound **4** and alkynes is superior only for the preparation of **G1OH** and **G1OTf**. For higher generations of monodendrons, the initial plan using enediyne **I** and triflates works better, even though excess of enediyne **I** had to be used and unreacted triflates were recovered.

Since it appeared that the use of enediyne (compound **I**) is unavoidable, we set out to optimize the reaction conditions. It is observed that the solvent plays an important role. The coupling reaction of aromatic iodides with alkynes took place readily in pure dry triethylamine without any other co-solvents. The heat released raised the reaction temperature rapidly. An external cooling bath had to be used to dissipate the energy. The reaction normally is complete in 1–2 h. However, if DMF was added as a co-solvent to enhance solubility, the reaction rate is significantly lower. No temperature increase was observed and extended reaction time was necessary to ensure complete transformation. For the coupling reaction of aryltriflates with alkynes such as **G0OTf** with trimethylsilylacetyelene, no reaction was detected by TLC after 4 h of reaction at 55°C when pure triethylamine was used as the only solvent. However, when DMF was injected into the mixture, the reaction proceeded smoothly and the reaction finished in 5 h. Clearly, DMF and triethylamine have distinctive effects on the reactivity of triflates and iodides. Reducing the amount of triethylamine used in the coupling reaction of triflates appears to be beneficial. Best results were obtained when a minimum amount of triethylamine (3–5 mol equiv. relative to monomer) was used. The modified procedure allows the use of considerably less thermally unstable enediyne monomer **I**. Although the yields did not increase considerably, the percentage of unreacted triflates decreased dramatically, for example, from 21 to 3%, for the preparation of **G2OH**.

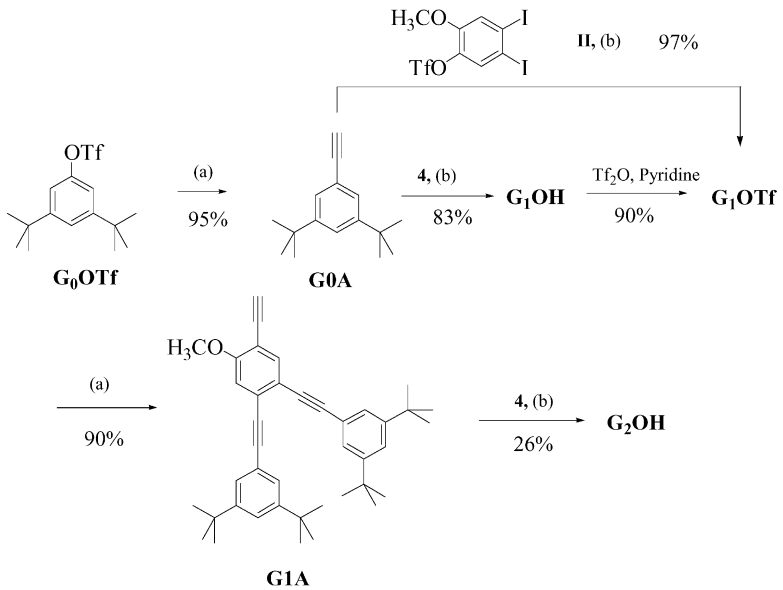


**Scheme 3.** Synthesis of monodendrons by an alternative route: (a) (i) trimethlysilylacetylene, $PdCl_2(PPh_3)_2$, $Et_3N$, DMF, 65°C, (ii) $Bu_4NF$, THF. (b) $PdCl_2(PPh_3)_2$, CuI, $Et_3N$, DMF, rt.

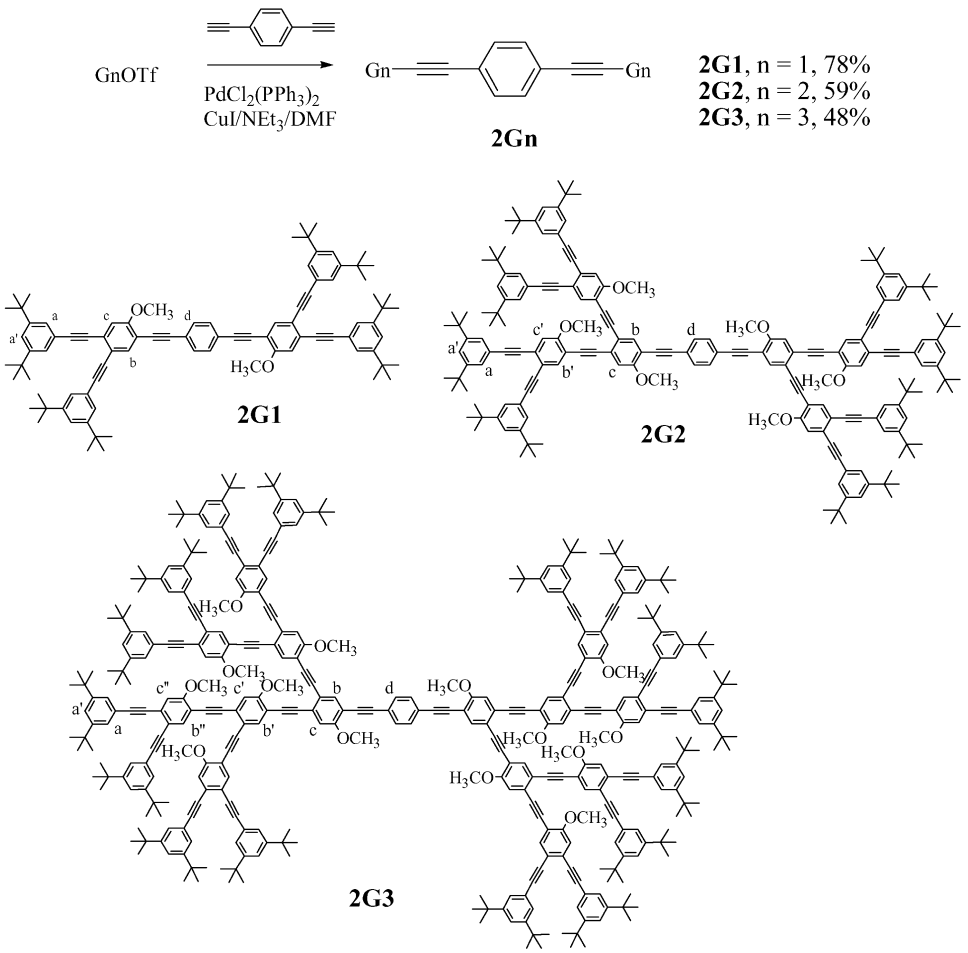


**Scheme 4.** Synthesis of didendron **2G*n***.

## 3. Synthesis of didendrons and tridendrons

Taking advantage of the triflate functional group at the core, a series of didendrons were synthesized by the coupling reaction of 1,4-diethynylbenzene with the **G*n*OTf** (Scheme 4). **2G1**, **2G2**, and **2G3** are synthesized in 78, 59 and 48%, respectively.

To synthesize tridendrons, trisubstituted benzene has to be prepared. 1,3,5-tribromobenzene was not reactive enough in the Sonogashira reaction, which would result in incomplete substitution and significant self-coupling side products. The reaction of 1,3,5-triethynylbenzene with **G1OTf** gave no desired product either, likely due to the sluggishness of the coupling reaction and the instability of triethynylbenzene. It is thus desirable to prepare 1,3,5-triiodobenzene.

There have been a few reports about the synthesis of 1,3,5-triiodobenzene which all involve the halogen exchange reaction of tribromobenzene with various iodination agents.[16–18] A mixture of homo and hetero-halogenated compounds are usually obtained, from which pure

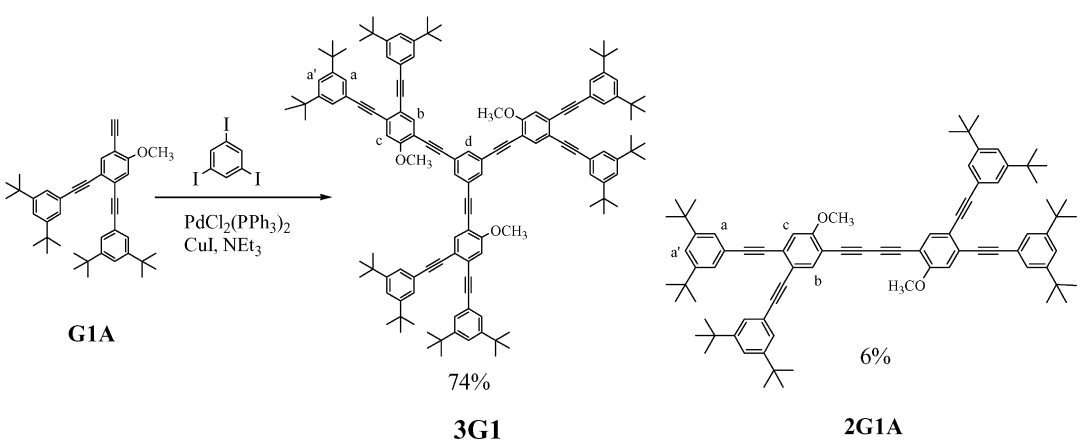


**Scheme 5.** Synthesis of G1 dendrimer **3G1**.

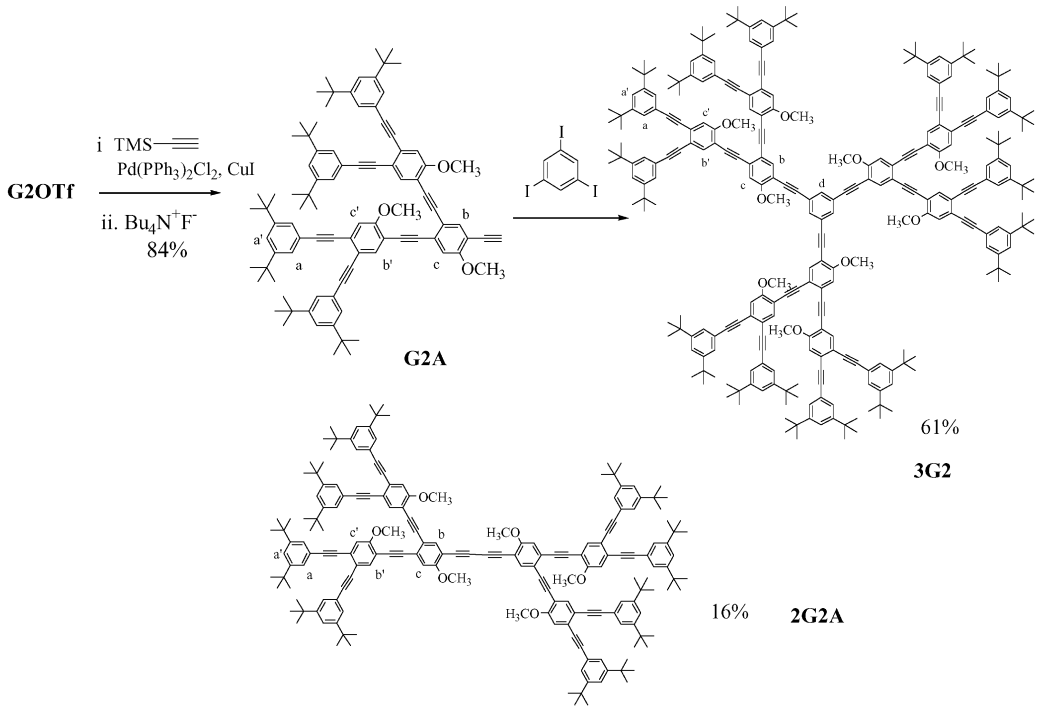


**Scheme 6.** Synthesis of **3G2**.

1,3,5-triiodobenzene is difficult to isolate. We prepared triiodobenzene from 3,5-diiodoaniline. By following a reference procedure that was designed to prepare triazene,[19] 1,3,5-triiodobenzene was prepared in good yields from 3,5-diiodoaniline. Thus, 3,5-diiodoaniline was treated with hydrochloric acid and then sodium nitrite. The resulting diazonium salt was decomposed with potassium iodide to give a precipitate, which was separated easily by filtration. It can be recrystallized from methylene chloride to give analytically pure product in about 80% yield. $^{1}$H NMR gives a singlet at 8.00 ppm. $^{13}$C NMR gives two carbon signals at 144.5 and 95.4 ppm. There were no impurities detectable by NMR spectroscopy. Elemental analysis confirms the high purity of the compound.

G1 dendrimer **3G1** was easily prepared by the Sonogashira coupling reaction of **G1A** and 1,3,5-triiodobenzene, as shown in Scheme 5. To ensure the complete coupling reaction, an excess of **G1A** was used, which resulted in a homocoupling side product **2G1A**. Even the strict exclusion of oxygen did not reduce the amount of this side product. **G2** dendrimer **3G2** was synthesized similarly (Scheme 6). The separation of the desired product **3G2** and side product **2G2A** required repetitive chromatography. For the synthesis of **3G3** dendrimer, we envisioned that the bulkiness of the acetylene terminated **G3** monodendron would cause a considerable drop in the yield of **3G3**. We also anticipated difficulties in separation of **3G3** and the homocoupling byproduct. The synthesis of **3G3** dendrimer was thus not attempted.

## 4. Structural characterizations

All generations of monodendrons, didendrons and tridendrons are soluble in most organic solvents including chloroform, THF and DMF. Their structures and purity are confirmed by thin-layer chromatography, elemental analysis, $^{1}$H and $^{13}$C NMR spectroscopy, and matrix-assisted

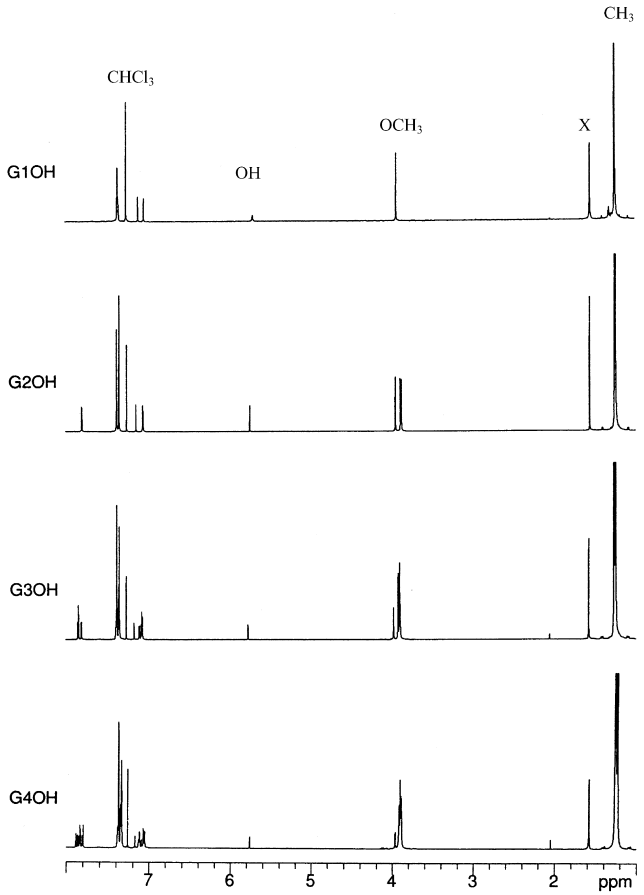


**Figure 1.** Stacked plot of $^{1}$H NMR spectra of **G*n*OH** in $CDCl_3$.

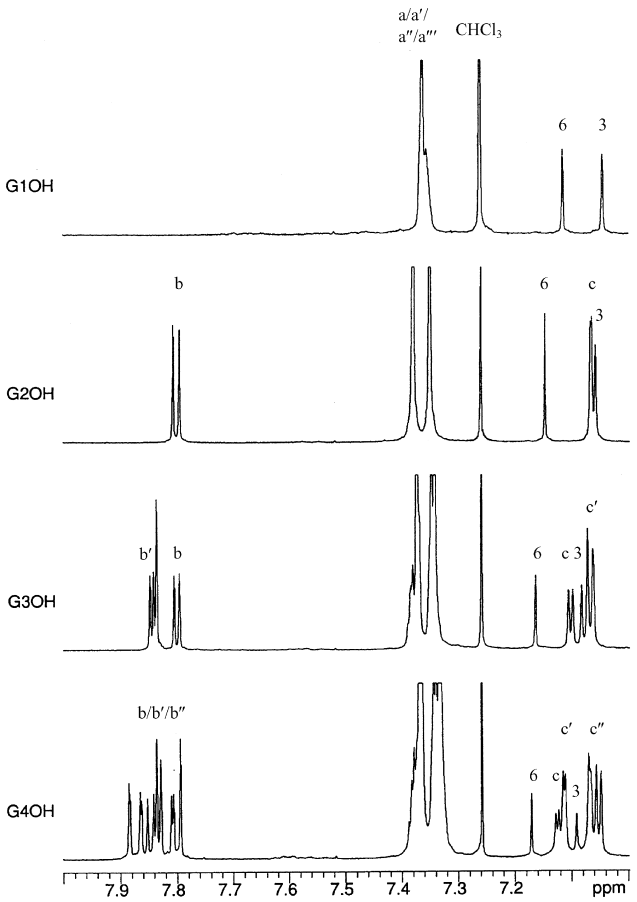


**Figure 2.** Stacked plot of aromatic regions of $^1$H NMR spectra of **G*n*OH** in $CDCl_3$.

laser desorption/ionization time-of-flight (MALDI-TOF) mass spectroscopy.

NMR spectra acquired in *d*-chloroform ($CDCl_3$) of **G*n*OH** give adequately dispersed signals. The signals are divided into four regions (Fig. 1). The signals at around $\delta$=1.26 ppm are due to methyl groups on the periphery. The signals at around $\delta$=3.88–3.97 ppm are due to hydrogens on methoxy groups at different layers of the monodendrons. The small singlet at approximately $\delta$=5.75–5.79 ppm is assigned to the hydrogen on the hydroxy group at the focal point. Its intensity rapidly diminishes compared to other parts of the spectrum for higher generation monodendrons and disappears for its corresponding triflate derivative. The aromatic regions provide the most important information since the aromatic rings are the building blocks in every monodendron. Fortunately, signals in the aromatic region are well dispersed (Fig. 2). The intense signals at around $\delta$=7.40–7.34 ppm are due to the aromatic hydrogens at the peripheral 3,5-di-*tert*-butylphenyl groups. The aromatic hydrogens on the benzene rings of inner layers are all singlets and divided into three groups. To help understand the spectrum in the aromatic region, it is useful to look at the spectrum for **G1OH**. The highly overlapped and broad signals at around $\delta$=7.40–7.34 ppm are due to the aromatic hydrogens at the peripheral phenyl rings. **G1OH** also gives two well-separated singlets at $\delta$=7.12, 7.05 ppm, which based on heteronuclear multiple-quantum correlation (HMQC) and heteronuclear multi-bond correlation (HMBC) experiments, are assigned to the H6 and H3 on the core benzene ring, respectively.

By analogy, the aromatic hydrogen H6 (see Scheme 1 for labeling) *ortho* to the hydroxy group at the focal point is found to be a singlet at 7.12, 7.15, 7.16 and 7.18 ppm for **G1OH**, **G2OH**, **G3OH** and **G4OH**, respectively (Fig. 2). It is interesting to note that this singlet gradually shifts downfield as the monodendron grows. This is most likely due to the more extended electron delocalization. After the hydroxy group is transformed to its triflate, this aromatic hydrogen resonance signal shifts significantly downfield to 7.42, 7.45, 7.46 and 7.48 ppm for **G1OTf**, **G2OTf**, **G3OTf** and **G4OTf**, respectively (Fig. 3). The aromatic hydrogen H3 *ortho* to the methoxy group on the central benzene ring is located as a singlet at 7.05, 7.06, 7.09 and 7.10 ppm for **G1OH**, **G2OH**, **G3OH** and **G4OH**, respectively.

The aromatic hydrogens next to the methoxy groups in the inner layers (c, c′ and c″ protons) are all located on the upfield side ranging from 7.06 to 7.18 ppm. **G1OH** has only a periphery and a core and does not have an inner layer, and thus shows no such proton signals. On the downfield side of the aromatic hydrogen region, with chemical shifts from 7.80 to 7.90 ppm, lies another group of hydrogens for all monodendrons except **G1OH**. These hydrogen signals are assigned to the aromatic hydrogens that are wedged between two triple bonds (b, b′ and b″ protons). For G1-acetylene compound **G1A**, where the hydroxy group of **G1OH** is replaced by an acetylene moiety, this signal (H6) shows up at $\delta$=7.68 ppm. **G2OH** has two such hydrogens and we observed two singlets at $\delta$=7.81 and 7.80 ppm. For the same

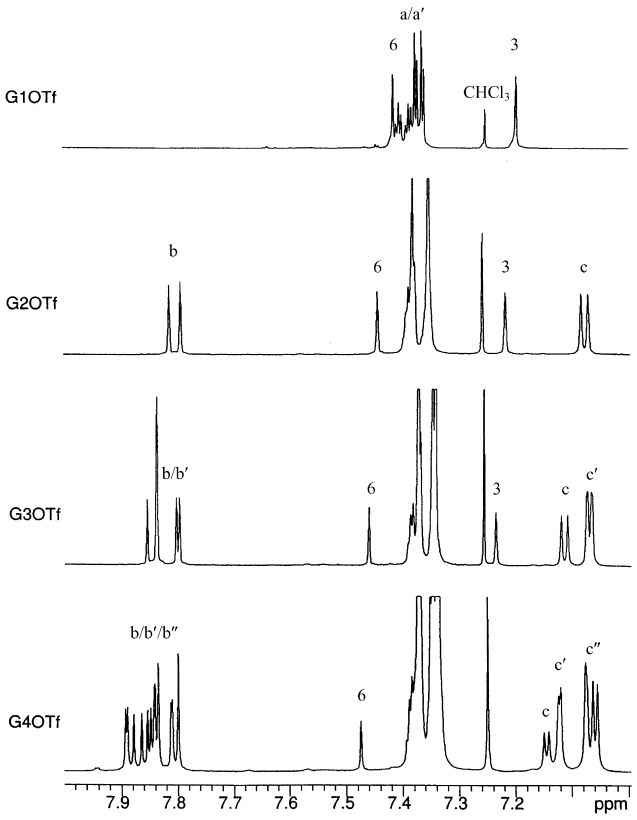


**Figure 3.** Stacked plot of aromatic regions of $^1$H NMR spectra of **G*n*OTf** in $CDCl_3$.

reason, **G3OH** and **G4OH** give 6 and 14 hydrogens, respectively, in that region with certain peak overlaps.

After the hydroxy group is transformed to its triflate, the aromatic hydrogens are better separated. Again, the two hydrogens H3 and H6 on the phenyl ring at the core are well separated from the rest of the signal and can be easily identified. The layer structures are visible by inspecting the locations and integrations of all the singlets in the upfield region from 7.04 to 7.18 ppm (Fig. 3). As discussed above, these signals are due to the hydrogens *ortho* to the methoxy groups (Hc, Hc′ and Hc″). It is obvious that the closer these hydrogens are to the core, the more deshielded they are. And also, the hydrogens in the same layers shift downfield as the sizes of the monodendrons increase.

The $^{1}$H NMR spectra of the didendrons show features similar to those of **G*n*OH** and **G*n*OTf**. For example, the signals corresponding to protons at the peripheral phenyl rings (protons a/a′) appear at 7.35–7.40 ppm. The aromatic protons *ortho* to the methoxyl group have chemical shift between 7.07 and 7.15 ppm. The protons *ortho* to both acetylene groups (protons c/c′/c″) appear as singlets between 7.70 and 7.90 ppm. The protons belonging to the center phenyl ring give a singlet at about 7.55 ppm for all three didendrons. The $^{13}$C NMR spectra of **2G*n*** didendrons provide important structural information as well. The signals in the range of 70–100 ppm correspond to alkynyl carbons. The $^{13}$C NMR spectra of **2G1**, **2G2**, and **2G3** show 6, 14, and 16 signals in that range respectively, consistent with their respective number of alkynyl carbons. The *t*-butyl carbons give two signals at 31.5 and 35.0 ppm, while the methoxy carbon appears at 56.3 ppm.

The $^{1}$H NMR spectrum of **3G1** gives two singlets at 7.72 and 7.73 ppm, as shown in Figure 4, which can be assigned to protons d and b (see Scheme 5 for the labeling) respectively. The fact that two singlets are present in this region, and that the integration ratio is nearly 1:1, confirms that the central phenyl ring was fully substituted with the same groups. LRFAB gives a mass of 1741, which is consistent with the calculated mass for $C_{129}H_{144}O_3$. For **2G1A**, its NMR spectrum is similar to that of **3G1** except it lacks the signal (d) corresponding to the central phenyl ring in **3G1**. The $^{13}$C NMR spectra of **3G1** show six alkynyl carbon signals (between 70 and 100 ppm) and 16 aryl carbon signals, which matches perfectly with its structure. The $^{13}$C NMR spectra of **2G1A**, which give six alkynyl

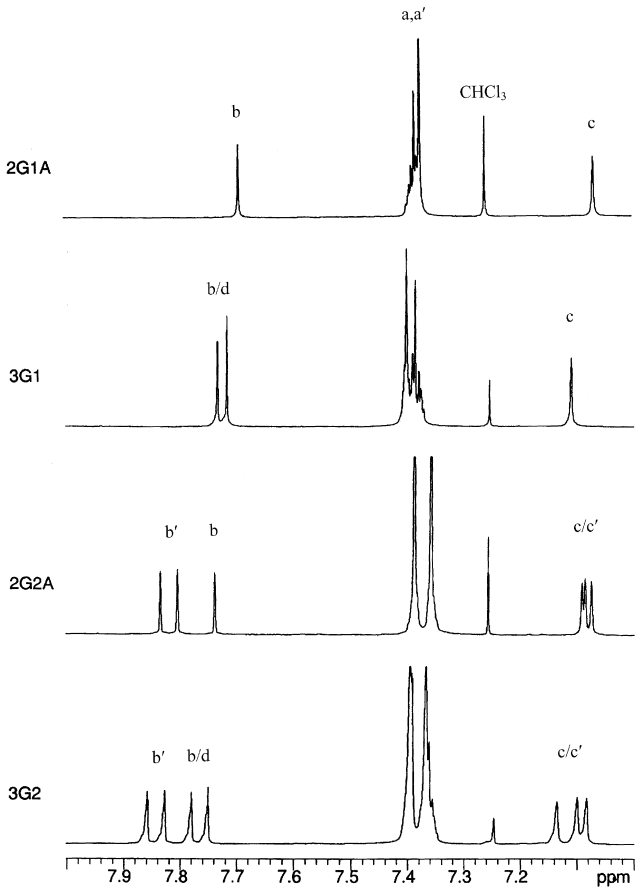


**Figure 4.** Stacked plot of aromatic regions of $^{1}$H NMR spectra of **3G*n*** and **2G*n*A** (*n*=1, 2) in $CDCl_3$.

**Table 1**. Optical properties of dendritic compounds

| Compound | $\lambda_{edge}^{ab}$ [a] (nm) | $\lambda_{max}^{ab}$ [b] (nm) | $\varepsilon_{max}$ [c] ($M^{-1}$ $cm^{-1}$) | $\lambda_{max}^{em}$ [d] (nm) | $\phi_{fl}$ [e] | $\tau$ [f] (ns) |
|---|---|---|---|---|---|---|
| **G1OH** | 356 | 283 | 48000 | 360, 374 (sh) | 0.40 | 1.7 |
| **G2OH** | 416 | 299 | 82500 | 417, 438 (sh) | 0.81 | 2.0 |
| **G3OH** | 440 | 310 | 171000 | 440, 466 (sh) | 0.70 | 1.9 |
| **G4OH** | 453 | 321 | 330000 | 452, 479 (sh) | 0.65 | 1.7 |
| **3G1** | 396 | 310 | 183000 | 401 | 0.80 | 1.7 |
| **3G2** | 432 | 324 | 328000 | 433, 455 (sh) | 0.84 | 1.8 |
| **2G1** | 418 | 382 | 75000 | 415, 437 (sh) | 0.80 | 0.79 |
| **2G2** | 442 | 304 | 160000 | 439, 463 (sh) | 0.73 | 1.1 |
| **2G3** | 454 | 308 | 330000 | 452, 478 (sh) | 0.71 | 1.2 |
| **G1A** | 376 | 276 | 48000 | 392 | 0.66 | 2.7 |
| **G2A** | 422 | 304 | 110000 | 425 | 0.84 | 2.4 |
| **2G1A** | 427 | 304 | 71000 | 422, 448 (sh) | 0.71 | 0.84, 2.8 |
| **2G2A** | 454 | 304 | 180000 | 450, 477 (sh) | 0.65 | 0.95 |

[a] Absorption band edge.
[b] Maximum absorption wavelengths.
[c] Molar extinction coefficients at the absorption maximum.
[d] Fluorescence emission wavelengths.
[e] Fluorescence quantum yields ($\phi_{fl}$).
[f] Fluorescence lifetimes.

carbon signals and 14 aryl carbon signals, are consistent with its structure as well.

The $^{1}$H NMR spectra of **3G2** and **2G2A** show well resolved signals as well. As shown in Figure 4, besides the two broad signals at 7.36–7.40 ppm which are due to protons in the peripheral phenyl rings, **3G2** gives seven well separated singlets, corresponding to the seven different types of aromatic protons in the inner-layer phenyl rings. **2G2A**, without the central phenyl ring, shows six singlets. The $^{13}$C NMR spectra of **3G2** and **2G2A** give 14 and 12 signals, respectively, in the range of 70–100 nm, consistent with the number of alkynyl carbons in their respective structure. The structures of **3G2** and **2G2A** are also confirmed by mass spectroscopy.

## 5. Optical and photophysical properties

The optical properties of all monodendrons, didendrons and tridendrons were studied by UV/Vis absorption, static-state and time-resolved fluorescence measurements. The photophysical properties of these compounds are collected in Table 1.

The absorption spectra of the **2G*n*** (didendrons) series are shown in Figure 5. The absorption spectra of the **G*n*OH** monodendrons are also shown for comparison. We note that

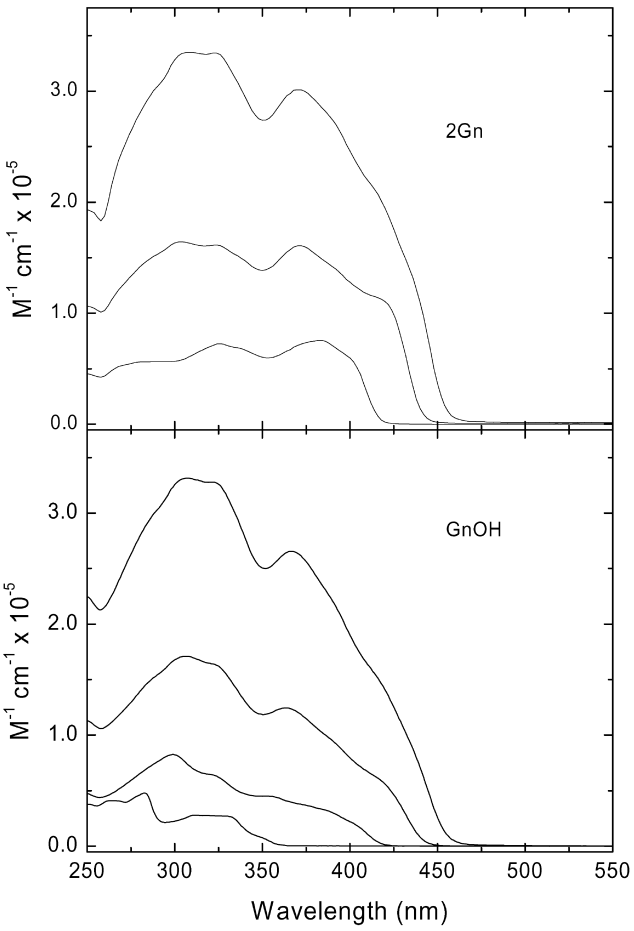


**Figure 5.** UV/Vis absorption spectra of **2G*n*** and **G*n*OH** in methylene chloride solutions.

a **2G*n*** didendron and **G(*n*+1)OH** monodendron have the same number of phenylacetylene units, and, thus, the same number of π-electrons. With increasing generation, the absorption band edges for **2G*n*** and **G*n*OH** shift to longer wavelengths and the molar extinction coefficient approximately doubles for each generation. It is worth noting that the **2G*n*** dendrimers exhibit nearly identical band edges to their **G(*n*+1)OH** dendrons. An inspection of the structures tells that these two series differ in the connectivity at the center of the molecule, where lower generation monodendrons join together. For **2G*n*** series, two **G*n*** monodendrons are connected to a benzene ring in the *para* positions, whereas for **G(*n*+1)OH** series, the **G*n*** monodendrons are joined at the *ortho* positions. Both *para* and *ortho* connectivities enable extended conjugation between monodendrons. The similar band edges indicate that the effective conjugation lengths are comparable for the two types of linkages.

Although **2G*n*** dendrimers and **G(*n*+1)OH** dendrons possess similar band edges, the **2G*n*** dendrimers have much stronger absorptions at wavelengths near the band edge. This can be clearly seen by comparing the absorption spectrum of **2G1** with that of **G2OH**. For **G2OH**, the absorption maximum is at 299 nm and the absorption declines gradually to its band edge. For **2G1**, the strongest absorption occurs at 382 nm and a much steeper absorption edge is observed. Although the effect is not as significant, when **2G2** and **2G3**, are compared to **G3OH** and **G4OH**, respectively, they show higher absorption strength at longer wavelengths as well. The absorption features at wavelengths near the band edge are likely associated with the central phenyl ring and its two extended π-conjugated arms. The linear (*para*) linkage may possess stronger transition moment than the bent (*ortho*) linkage, which contributes to the stronger absorption of **2G*n***. This argument is supported by the fluorescence lifetime measurements where shorter fluorescence lifetimes are observed for **2G*n*** dendrimers (see Table 1).

The steady-state fluorescence emission spectra of **2G*n*** and **G*n*OH** are shown in Figure 6. The fluorescence spectra of **2G*n*** and **G(*n*+1)OH** are nearly identical with respect to

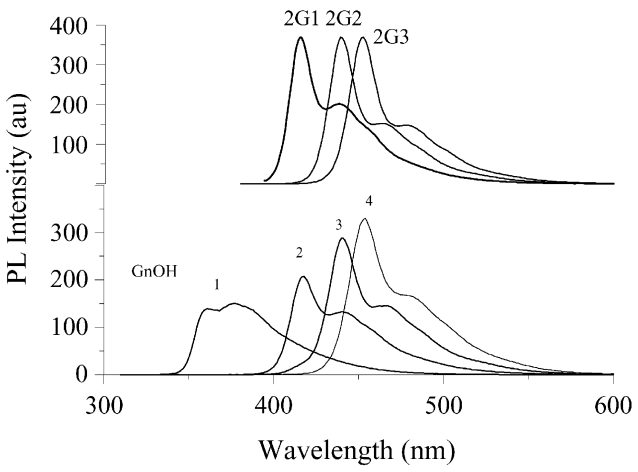


**Figure 6.** Fluorescence spectra of **2G*n*** and **G*n*OH** in methylene chloride solutions. The number above each curve in the bottom figure corresponds to n in GnOH.

both the peak position and the emission profile. With increasing generation, the emission wavelength red shifts. For each member of the **2G*n*** and **G(*n*+1)OH** series, the emission profiles remain independent of the excitation wavelengths, indicating that rapid and efficient energy transfer occurs from shorter branches to the main linear conjugated branch.

As shown in Table 1, both **2G*n*** and **G*n*OH**, in general, show high fluorescence quantum yields. **2G1** exhibits the highest quantum yield of 80%, comparable to that of **G2OH** (81%) within the experimental error. The quantum yields decrease slightly with increasing generations, with **2G3** exhibiting a quantum yield of 70%. The quantum yields for **2G2** and **2G3** are slightly higher than those of **G3OH** and **G4OH**, respectively, presumably due to the shorter radiative lifetime of the emitting state in the **2G*n*** series, which enhances relaxation to the ground state via fluorescence over competing non-radiative processes.

Figure 7 shows the absorption and fluorescence emission spectra of **2G1A** and **2G2A**. Structurally, for **2G*n*A**, monodendrons are connected by forming a single bond between two triple bonds of **G*n*A**, while for the **2G*n*** series, monodendrons are linked to a central benzene ring at *para* positions. As shown in Figure 7 and Table 1, the absorption spectrum of **2G1A** displays two intense bands at wavelengths as high as 382 and 406 nm. Compared to the absorption spectrum of **2G1**, the spectrum of **2G1A** exhibits slightly higher intensities at short wavelengths and lower intensities at longer wavelengths. The absorption band edge for **2G1A** ($\lambda_{edge}$) is red shifted by 9 nm with respect to **2G1**, indicating that the π-delocalization through a diacetylene bridge is somewhat more efficient than a diethynylphenyl bridge. This effect is more evident in the higher generation **2G2A**. As shown in Figure 7, the absorption band edge for **2G2A** extends to 454 nm, comparable to that of **2G3**, which is more than twice as large as **2G2A** in terms of the molecular weight. **2G1A** and **2G2A** are also highly fluorescent materials with fluorescence quantum yields around 70% (Table 1). While **2G*n*A** have similar fluorescence quantum yields to that of **2G*n***, their fluorescence life times are significantly shorter. This again may reflect the fact that **2G*n*A** have longer conjugation lengths, resulting in stronger transition dipoles.

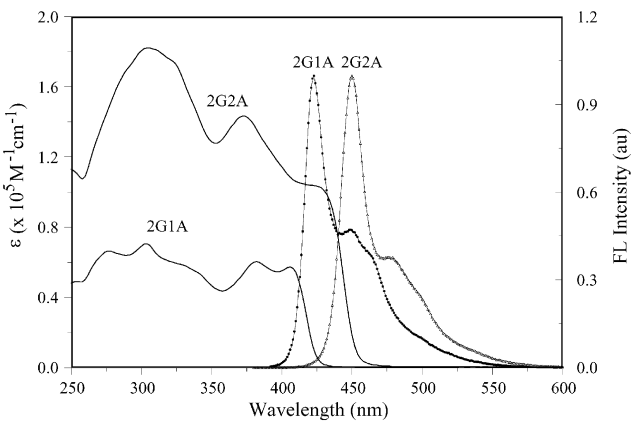


**Figure 7.** UV/Vis absorption and fluorescence spectra of **2G1A** and **2G2A**.

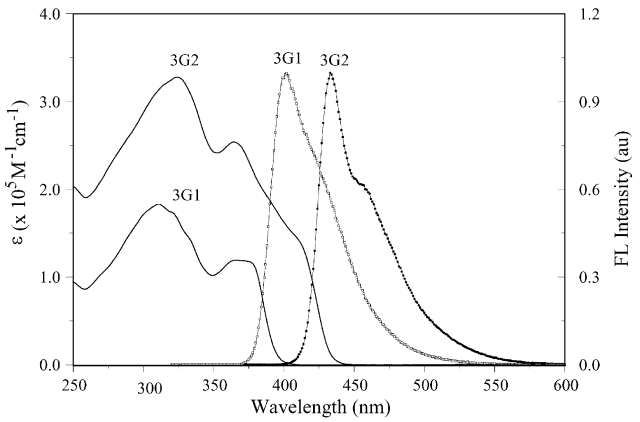


**Figure 8.** UV/Vis absorption and fluorescence spectra of **3G1** and **3G2**.

The optical properties of tridendrons (**3G1** and **3G2**) are shown in Figure 8. With dendrons linked at the *meta*-positions, π-conjugation is not expected to significantly extend across branches in different monodendrons. Indeed, the absorption band edges for **3G1** and **3G2** are at shorter wavelengths than that of **2G1** and **2G2**, but at longer wavelengths that that of **G1OH** and **G2OH**. The red shift of **3G1** with respect to **G1OH** (40 nm; 2837 $cm^{-1}$) is much larger than the red shift of **3G2** with respect to **G2OH** (16 nm; 890 $cm^{-1}$). For the **3G*n*** series, each monodendron interacts with the central benzene ring, which provides an additional pathway for π-electron delocalization. The additional pathway has a larger effect in the smaller (**3G1**) dendrimer. Both **3G1** and **3G2** exhibit high fluorescence quantum yields of over 80%. Clearly, coupling the three dendrons at the *meta*-position of the central benzene ring provides enough spatial isolation so that interactions between the dendrons that potentially reduce fluorescence quantum efficiency are not significant.

## 6. Conclusions

An improved synthetic approach to the building block molecule and an alternative route to unsymmetrical PA monodendrons are reported. A series of dendrimers containing two or three such PA monodendrons are synthesized. These dendrimers exhibit broad absorptions and large extinction coefficients, and show efficient energy transfer from the shorter branches to the longest conjugated branch. All these rigid dendrimers are highly fluorescent materials with quantum yields over 70%, suggesting that they are promising materials for application in molecular photonics.

## 7. Experimental

### 7.1. General

All reagents and solvents were obtained from either Aldrich or Fisher and were used as received unless otherwise stated. Anhydrous THF and acetonitrile were distilled prior to use from sodium metal/benzophenone. Triethylamine was distilled from calcium hydride prior to use. All air and moisture-sensitive reactions were carried out under $N_2$ atmosphere.

$^1$H NMR spectra were recorded on Varian Unity 400 MHz. UV–VIS absorption spectra were recorded using a Hewlett–Packard 8452A diode array spectrophotometer. The fluorescence emission spectra were measured using a Shimadzu RF-5301PC spectrofluorophotometer. Fluorescence quantum yields were determined using quinine sulfate in 1N $H_2SO_4$ ($\phi_{fl}\approx0.55$) as the standard.[20] Time-dependent fluorescence measurements were performed using the technique of time-correlated single photon counting (TCSPC).

The preparations of compounds **G*n*OH** ($n$=1–4) and **G*n*OTf** ($n$=0–4) were reported previously.[7]

**$G_1$OTf** by the alternative route. Triethylamine (50 mL) and DMF (30 mL) were added into a mixture containing compound **II** (15.5 g, 30.5 mmol), (3,5-di-*tert*-butylphenyl)acetylene **GoA** (14.5 g, 67.6 mmol), $Pd(PPh_3)_2Cl_2$ (1.03 g, 1.47 mmol) and copper(I) iodide (0.119 g, 0.623 mmol). The resulting mixture was stirred at room temperature for 1.5 h and then poured into 50 mL of 3 M hydrochloric acid. After extraction with methylene chloride (3×100 mL), the combined organic extracts were washed with water (3×50 mL) and brine (50 mL), dried over anhydrous sodium sulfate and evaporated in vacuo to give a red brown oil, which was then purified by column chromatography eluting with hexane, and then hexane/ethyl acetate (12:1) to give 20.1 g of the title compound as white crystals (97% yield). The structural characterization data for **G1OTf** have previously been reported.

**7.1.1. 1,3-Bis(1,1-dimethylethyl)-5-ethynylbenzene (G0A).** A mixture of 3,5-di-*tert*-butylphenyl trifluoromethanesulfonate **G0OTf** (1.00 g, 2.96 mmol), trimethylsilylacetylene (0.50 mL, 3.54 mmol), $Pd(PPh_3)_2Cl_2$ (0.119 g, 0.169 mmol), triethylamine (2.0 mL) and DMF (5.0 mL) was stirred under nitrogen at 50°C overnight. The reaction mixture was slowly poured into cold hydrochloric acid (3 M) and was then extracted with methylene chloride. The organic extracts were washed with water and brine, dried over anhydrous sodium sulfate and the solvent was then evaporated. The resulting black solid was then purified by passing through a silica gel column eluting with hexane to yield 0.84 g of [[3,5-bis(1,1-dimethylethyl)phenyl]-ethynyl]trimethylsilane (**G0A-TMS**) as white crystals (99%, mp 133–135°C). $^1$H NMR (250 MHz, $CDCl_3$) $\delta$ 7.38 (s, 1H), 7.33 (s, 2H), 1.32 (s, 18H), 0.27 (s, 9H). **G0A-TMS** was disilylated by adding a sample of $Bu_4NF$ (0.27 g, 0.857 mmol) to a THF solution of **G0A-TMS** (0.221 g, 0.772 mmol in 2.0 mL of THF). The solution was stirred at room temperature for 30 min and poured into water. It was extracted with methylene chloride. The organic extracts were washed with water, dried over anhydrous sodium sulfate and evaporated in vacuo to give a yellow solid. It was then purified by passing through a short silica gel column, eluting with hexane to afford 0.150 g of **G0A** as a white solid (90%, mp 86–87°C). $^1$H NMR (250 MHz, $CDCl_3$) $\delta$ 7.42 (t, 1H, $J$=2.5 Hz), 7.35 (d, 2H, $J$=2.5 Hz), 3.03 (s, 1H), 1.31 (s, 18H). $^{13}$C NMR (62.5 MHz, $CDCl_3$) $\delta$ 151.1, 126.6, 123.5, 121.2, 85.1, 76.0, 35.0, 31.5. Anal. calcd for $C_{16}H_{22}$: C, 89.65; H, 10.35. Found: C, 89.47; H, 10.56.

The synthetic procedures for **G1A** and **G2A** are similar to those of **G0A**.

**7.1.2. Compound G1A.** Yield: 91%. Mp 187–188°C. $^1$H NMR (400 MHz, $CDCl_3$) $\delta$ 7.68 (s, 1H), 7.39–7.36 (m, 6H), 7.08 (s, 1H), 3.95 (s, 3H), 3.38 (s, 1H), 1.26 (m, 36H). $^{13}$C NMR (100 MHz, $CDCl_3$) $\delta$ 159.8, 151.1, 151.0, 137.6, 128.1, 126.2, 126.0, 123.5, 123.1, 122.4, 122.0, 119.0, 113.8, 111.8, 96.7, 93.9, 87.0, 86.0, 82.9, 79.3, 56.3, 35.0, 31.5. Anal. calcd for $C_{41}H_{48}O$: C, 88.44; H, 8.69. Found: C, 88.32; H, 8.74.

**7.1.3. Compound G2A.** Yield: 94%. $^1$H NMR (400 MHz, $CDCl_3$) $\delta$ 7.88 (s, 1H), 7.83 (s, 1H), 7.74 (s, 1H), 7.42–7.39 (m, 12H), 7.12–7.11 (m, 3H), 3.99–3.93 (m, 9H), 3.43 (s, 1H), 1.30–1.29 (m, 72H). $^{13}$C NMR (100 MHz, $CDCl_3$) $\delta$ 160.0, 159.5, 159.3, 151.0 (m), 137.9, 137.5, 137.2, 127.9, 127.6, 127.3, 126.1, 126.0, 123.4, 123.3, 123.0, 122.9, 122.6, 122.5, 122.2, 122.1, 119.0, 118.9, 118.6, 114.1, 113.9, 113.8, 113.4, 112.8, 112.2, 96.9, 96.5, 94.0, 93.8 (two overlapped peaks), 93.0, 91.1, 88.5, 87.3, 87.2, 86.4, 86.3, 83.1, 79.2, 56.4, 35.0, 31.5. Anal. calcd for $C_{91}H_{100}O_3$: C, 88.02; H, 8.12. Found: C, 87.76; H, 8.24.

**7.1.4. Compound 2G1.** The mixture containing 1,4-diethynylbenzene (0.0467 g, 0.370 mmol), **$G_1$OTf** (0.507 g, 0.745 mmol), $Pd(PPPh_3)_2Cl_2$ (0.0409 g, 0.0583 mmol), copper(I) iodide (0.0024 g, 0.0126 mmol), triethylamine (5.0 mL) and DMF (5.0 mL) was stirred under $N_2$ at 63°C for 14 h. The reaction mixture was slowly poured into hydrochloric acid (3 M) and was then extracted with methylene chloride. The organic extracts were washed with water and brine, dried over anhydrous sodium sulfate and the solvent was then evaporated. The resulting solid was purified by chromatography eluting with hexane to yield the title compound as a white solid (0.350 g, 78% yield). $^1$H NMR (400 MHz, $CDCl_3$) $\delta$ 7.72 (s, 2H), 7.54 (s, 4H), 7.40–7.38 (m, 12H), 7.10 (s, 2H), 3.97 (s, 6H), 1.27 (s, 72H). $^{13}$C NMR (62.5 MHz, $CDCl_3$) $\delta$ 159.2, 151.1, 150.9, 139.7, 137.0, 131.8, 127.5, 126.2, 126.1, 123.5, 123.0, 122.5, 122.1, 119.0, 113.8, 112.9, 96.7, 95.1, 93.8, 87.2, 87.1, 86.2, 56.3, 35.0, 31.5. Anal. calcd for $C_{88}H_{98}O_2$: C, 88.99; H, 8.32. Found: C, 88.71; H, 8.40. MS (LRFAB) calcd for $C_{88}H_{98}O_2$ 1187.7, found 1188.

The synthetic procedure for **2G2** and **2G3** is similar to that of **2G1**.

**7.1.5. Compound 2G2.** Yield: 59%. $^1$H NMR (400 MHz, $CDCl_3$) $\delta$ 7.85 (s, 2H), 7.81 (s, 2H), 7.77 (s, 2H), 7.57 (s, 4H), 7.39–7.36 (m, 24H), 7.12 (s, 2H), 7.10 (s, 2H), 7.08 (s, 2H), 3.99 (s, 6H), 3.91 (s, 12H), 1.27–1.26 (m, 144 H). $^{13}$C NMR (62.5 MHz, $CDCl_3$) $\delta$ 159.4, 159.3, 150.9, 137.4, 137.2, 132.6, 131.8, 127.8, 127.3, 127.1, 126.1, 126.0, 123.3, 123.0, 122.5, 122.4, 122.1, 122.0, 118.9, 118.8, 118.6, 114.0, 113.8, 113.4, 113.3, 112.9, 96.8, 96.5, 95.4, 94.0, 93.9, 93.8, 93.3, 91.0, 88.4, 87.3, 87.2, 87.0, 86.4, 86.3, 56.3, 34.9, 31.5. Anal. calcd for $C_{188}H_{202}O_6C$, 88.28; H, 7.96. Found: C, 88.05; H, 8.13. MS (LRFAB) calcd for $C_{188}H_{202}O_6$ 2557.5, found 2557.

**7.1.6. Compound 2G3.** Yield: 48%. $^1$H NMR (400 MHz, $CDCl_3$) $\delta$ 7.88–7.78 (m, 14H), 7.57 (s, 4H), 7.38–7.35 (m,

48H), 7.13–7.07 (m, 14H), 4.00–3.91 (m, 42H), 1.26–1.24 (m, 288 H). $^{13}$C NMR (62.5 MHz, $CDCl_3$) $\delta$ 159.7, 159.6, 159.4, 159.3, 150.9, 137.8, 137.5, 137.2, 132.6, 131.8, 129.0, 127.8, 127.7, 127.3, 127.2, 127.1, 126.8, 126.4, 126.1, 125.9, 123.3, 122.9, 122.5, 122.4, 122.1, 118.9, 118.8, 118.6, 118.4, 114.1, 113.8, 113.3, 96.7, 96.4, 94.3, 94.1, 94.0, 93.9, 93.8, 93.5 (m), 90.9, 88.5, 88.4, 87.2, 86.4, 86.3, 56.4, 34.9, 31.5. Anal. calcd for $C_{388}H_{410}O_{14}$ C, 87.97; H, 7.80. Found C, 87.43; H, 8.07. MS (LRFAB) calcd for $C_{388}H_{410}O_{14}$ 5297.2, found 5298.

**7.1.7. 1,3,5-Triiodobenzene.** To a solution of 3,5-diiodoaniline (34.1 mmol) in acetonitrile (60 mL) was added 20 mL of water, 20 mL of concentrated hydrochloric acid. The resulting milk like mixture was cooled to 0°C. To this suspension was added dropwise a cold solution of sodium nitrite (2.82 g, 40.9 mmol) in 15 mL of water. A solution of KI (7.20 g, 43.4 mmol) was then added and the resulting mixture was stirred overnight. The precipitate was filtered and then recrystallized from methylene chloride to give the product as pink needles (79%. Mp 181–182°C). $^1$H NMR (400 MHz, $CDCl_3$) $\delta$ 8.00 (s, 3H). $^{13}$C NMR (100 MHz, $CDCl_3$) $\delta$ 144.5, 95.4. Anal. calcd for $C_6H_3I_3$: C, 15.81; H, 0.66. Found: C, 15.83; H, 0.70.

**7.1.8. Compound 3G1.** The mixture containing 3,5-triiodobenzene (0.0528 g, 0.116 mmol) and **G1A** (0.211 g, 0.380 mmol), $Pd(PPh_3)_2Cl_2$ (0.0124 g, 0.0184 mmol), copper(I) iodide (0.0011 g, 0.00578 mmol) and triethylamine (10 mL) were stirred at room temperature for 8.5 h and was then poured into hydrochloric acid (3 M). After extraction with methylene chloride, the organic extracts were washed with water and dried over anhydrous sodium sulfate and the solvent was then evaporated. The resulting crude product was purified by flash chromatography using hexane as the eluent to give 0.161 g of **3G1** as a yellow powder (74% yield). $^1$H NMR (400 MHz, $CDCl_3$) $\delta$ 7.73 (s, 3H), 7.72 (s, 3H), 7.40–7.38 (m, 18H), 7.11 (s, 3H), 3.99 (s, 9H), 1.27 (m, 108 H). $^{13}$C NMR (100 MHz, $CDCl_3$) $\delta$ 159.2, 150.9, 150.7, 136.8, 134.3, 127.5, 126.0, 125.8, 124.0, 123.2, 122.8, 122.3, 121.9, 118.8, 113.79, 112.5, 96.5, 93.7, 93.5, 87.0, 86.1, 86.0, 56.1, 34.8, 31.3 (two peaks). MS (LRFAB) calcd for $C_{129}H_{144}O_3$ 1741.1, found 1741.

**7.1.9. 3G1 side product (2G1A).** A yellow solid (0.0115 g) was separated as a side product after flash column chromatography in the above reaction. Yield: 6%. $^1$H NMR (400 MHz, $CDCl_3$) $\delta$ 7.69 (s, 2H), 7.40–7.38 (m, 12H), 7.07 (s, 2H), 4.00 (s, 6H), 1.27 (m, 72H). $^{13}$C NMR (100 MHz, $CDCl_3$) $\delta$ 160.6, 151.1, 151.0, 137.7, 128.3, 126.2, 126.1, 123.5, 123.1, 122.4, 122.0, 119.1, 113.9, 111.8, 97.3, 94.0, 87.2, 86.0, 79.7, 78.8, 56.3, 35.0 (m, two overlapped peaks), 31.5 (m, two overlapped peaks). MS (LRFAB) calcd for $C_{82}H_{94}O_2$ 1111.6, found 1112.

**7.1.10. Compound 3G2.** The synthetic procedure is similar to that of **3G1**. Yield: 61%. Yellow powder. $^1$H NMR (400 MHz, $CDCl_3$) $\delta$ 7.86 (s, 3H), 7.82 (s, 3H), 7.78 (s, 3H), 7.75 (s, 3H), 7.40–7.36 (m, 36H), 7.13 (s, 3H), 7.10 (s, 3H), 7.08 (s, 3H), 4.01 (s, 9H), 3.92 (m, 18H), 1.27 (m, 216 H). $^{13}$C NMR (100 MHz, $CDCl_3$) $\delta$ 159.4, 159.3, 159.2, 150.8 (m, three overlapped peaks), 137.2, 137.1, 137.0, 134.4, 127.6, 127.1, 127.0, 125.9, 125.8, 124.0, 123.2, 123.1, 122.8, 122.7, 122.4, 122.3, 122.0, 121.9, 118.8, 118.7, 118.4, 113.9, 113.7, 113.6, 113.3, 113.0, 112.8, 96.6, 96.3, 93.9, 93.8, 93.7, 93.6, 93.1, 90.9, 88.2, 87.2, 87.1 86.2, 86.1, 86.0, 56.2 (m), 34.7, 31.3. MS (LRFAB) calcd for $C_{279}H_{300}O_9$ 3797.2, found 3798.

**7.1.11. 3G2 side product (2G2A).** A yellow solid (0.0343 g) was separated as a side product after flash column chromatography of the above reaction. Yield: 16%. $^1$H NMR (400 MHz, $CDCl_3$) $\delta$ 7.84 (s, 2H), 7.81 (s, 2H), 7.74 (s, 2H), 7.39–7.36 (m, 24H), 7.09 (m, 6H), 3.98 (s, 6H), 3.91 (m, 12H), 1.27 (m, 144 H). $^{13}$C NMR (100 MHz, $CDCl_3$) $\delta$ 160.8, 159.5, 159.4, 151.0, 138.1, 137.5, 137.2, 135.4, 135.3, 135.2, 131.5, 128.4, 128.0, 127.9, 127.4, 126.2, 126.0, 123.4, 123.3, 123.0, 122.9, 122.6, 122.5, 122.2, 122.1, 119.0, 118.9, 118.7, 114.1, 113.9, 113.8, 113.4, 112.8, 112.2, 94.0 (m, three overlapped peaks), 93.0, 91.7, 88.5, 87.3, 87.2, 86.4, 86.3, 79.9, 78.8, 56.4 (m), 35.0 (m), 31.5. MS (MALDI) calcd for $C_{182}H_{198}O_6$ 2479.5, found 2479.7.

## Acknowledgements

This work is supported by the Office of Naval Research and the Defense Advanced Research Project Agency.

## References

1. (a) Newkome, G. R.; Moorefield, C. N.; Vögtle, F. *Dendritic Molecules: Concepts, Syntheses, Perspectives*; VCH: Weinheim, 1996. (b) Fréchet, J. M. J.; Hawker, C. J. Synthesis and Properties of Dendrimers and Hyperbranched Polymers. *Comprehensive Polymer Science*; Aggarwal, S. L., Russo, S., Eds.; Pergamon: Oxford, 1996; 2nd Suppl. (c) Fischer, M.; Vögtle, F. *Angew. Chem., Int. Ed. Engl.* **1999**, *38*, 884–905. (d) Smith, D. K.; Diederich, F. *Chem. Eur. J.* **1998**, *4*(8), 1353–1361. (e) Tomalia, D. A.; Naylor, A. M.; Goddart, W. A., III. *Angew. Chem., Int. Ed. Engl.* **1990**, *29*, 138–175. (f) Zeng, F.; Zimmerman, S. C. *Chem. Rev.* **1997**, *97*, 1681–1712. (g) Grayson, S. M.; Fréchet, J. M. J. *Chem. Rev.* **2001**, *101*, 3819–3867.
2. (a) Denti, G.; Campagna, S.; Serroni, S.; Ciano, M.; Balzani, V. *J. Am. Chem. Soc.* **1992**, *114*, 2944–2950. (b) Stewart, G. M.; Fox, M. A. *J. Am. Chem. Soc.* **1996**, *118*, 4354–4360. (c) Balzani, V.; Campagna, S.; Denti, G.; Juris, A.; Serroni, S.; Venturi, M. *Acc. Chem. Res.* **1998**, *31*, 26–34. (d) Sato, T.; Jiang, D.-L.; Aida, T. *J. Am. Chem. Soc.* **1999**, *121*, 10658–10659. (e) Schenning, A. R. H. J.; Peeters, E.; Meijer, E. W. *J. Am. Chem. Soc.* **2000**, *122*, 4489–4495. (f) Gust, D.; Moore, T. A.; Moore, A. L. *Acc. Chem. Res.* **2001**, *34*, 40–48.
3. (a) Adronov, A.; Frechet, J. M. J. *Chem. Commun.* **2000**, 1701–1710. (b) Gilat, S. L.; Adronov, A.; Fréchet, J. M. J. *Angew. Chem. Int. Ed.* **1999**, *38*, 1422–1427. (c) Gilat, S. L.; Adronov, A.; Fréchet, J. M. J. *J. Org. Chem.* **1999**, *64*(20), 7474–7484. (d) Adronov, A.; Gilat, S. L.; Frechet, J. M. J.; Ohta, K.; Neuwahl, F. V. R.; Fleming, G. R. *J. Am. Chem. Soc.* **2000**, *122*(6), 1175–1185.
4. Devadoss, C.; Bharathi, P.; Moore, J. S. *J. Am. Chem. Soc.* **1996**, *118*(40), 9635–9644.
5. (a) Moore, J. S. *Acc. Chem. Res.* **1997**, *30*, 402. (b) Berresheim,

A. J.; Müllen, K. *Chem. Rev.* **1999**, *99*, 1747. (c) Miller, T. M.; Neenan, T. X.; Zayas, R.; Bair, H. E. *J. Am. Chem. Soc.* **1992**, *114*, 1018. (d) Deb, S.; Madux, T. M.; Yu, L. *J. Am. Chem. Soc.* **1997**, *119*, 9079. (e) Meier, H.; Lehmann, M.; Yu, L. *Angew. Chem., Int. Ed. Engl.* **1998**, *37*, 643.

6. Shortreed, M. R.; Swallen, S. F.; Shi, Z.; Tan, W.; Xu, Z.; Devadoss, C.; Moore, J.; Kopelman, S. R. *J. Phys. Chem. B* **1997**, *101*, 6318.
7. Peng, Z.; Pan, Y.; Yu, B.; Zhang, J. *J. Am. Chem. Soc.* **2000**, *122*(28), 6619–6623.
8. Melinger, J. S.; Pan, Y.; Kleiman, V. D.; Peng, Z.; Davis, B. L.; McMorrow, D.; Lu, M. *J. Am. Chem. Soc.* **2002**, *124*(40), 12002–12012.
9. Wang, J.; Pan, Y.; Lu, M.; Peng, Z. *J. Org. Chem.* **2002**, *67*(22), 7781.
10. Bhatt, M. V. *J. Organomet. Chem.* **1978**, *156*, 221–226.
11. (a) Sala, T.; Sargent, M. V. *J. Chem. Soc., Perkin Trans. 1* **1979**, *10*, 2593–2598. (b) Banwell, M. G.; Flynn, B. L.; Stewart, S. G. *J. Org. Chem.* **1998**, *63*(24), 9139–9144.
12. Bergman, R. G. *Acc. Chem. Res.* **1973**, *6*(1), 25–31.
13. Shultz, D. A.; Gwaltney, K. P.; Lee, H. *J. Org. Chem.* **1998**, *63*(12), 4034–4038.
14. Sonogashira, K.; Tohda, Y.; Hagihara, N. *Tetrahedron Lett.* **1975**, 4467.
15. Lu, M.; Pan, Y.; Peng, Z. *Tetrahedron Lett.* **2002**, *43/44*, 7903.
16. Godt, A.; Franzen, C.; Veit, S.; Enkelmann, V.; Pannier, M.; Jeschke, G. *J. Org. Chem.* **2000**, *65*(22), 7575–7582.
17. (a) Schoeberl, U.; Magnera, T. F.; Harrison, R. M.; Fleischer, F.; Pflug, J. L.; Schwab, P. F. H.; Meng, X.; Lipiak, D.; Noll, B. C.; Allured, V. S.; Rudalevige, T.; Lee, S.; Michl, J. *J. Am. Chem. Soc.* **1997**, *119*(17), 3907–3917. (b) Yang, S. H.; Li, C. S.; Cheng, C. H. *J. Org. Chem.* **1987**, *52*(4), 691–694.
18. Rot, N.; Bickelhaupt, F. *Organometallics* **1997**, *16*(23), 5027–5031.
19. Moore, J. S.; Xu, Z. *Macromolecules* **1991**, *24*(21), 5893–5894.
20. Demas, J. N.; Crosby, G. A. *J. Phys. Chem.* **1971**, *75*, 991–1024.